Journal of Optoelectronics and Advanced Materials Vol. 5, No. 3, September 2003, p. 755 – 761

# STUDY OF TRANSPARENT FERROELECTRIC THIN FILMS BY OPTICAL REFLECTOMETRY AND ELLIPSOMETRY

I. Aulika*, V. Zauls, K. Kundzins, M. Kundzins, S. Katholy[a]

Institute of Solid State Physics, University of Latvia, Riga, Latvia
[a]Institute of Physics, University of Potsdam, Potsdam, Germany

A method of analyzing variable-angle null-ellipsometry and reflectometry measurement data is proposed for barium titanate $BaTiO_3$ (BT), lead zirconate titanate $PbZr_{0,47}Ti_{0,53}O_3$ (PZT) and lead magnesium niobate $Pb(Mn_{0,33}Nb_{0,67})O_3$ (PMN) thin films grown on $Si/SiO_2/Ti/Pt$, $Si/TiO_2/Pt$, substrates by laser ablation, sol-gel and rf sputtering. The refractive and absorption coefficients of the samples are determined in the phonon energy range of 1.65 – 3.53 eV. The variation of the optical property in BT thin films of various thickness was observed and explained by the characteristic film structure.

(Received July 10, 2003; accepted July 31, 2003)

*Keywords*: Ellipsometry, Reflectometry, Refractive index, Absorption coefficient

## 1. Introduction

Ferrolectric thin films have attracted much attention due to their potential applications such as high dielectric constant capacitors, non-volatile memories, infrared sensors and electro-optic devices. Their ferroelectric and dielectric properties have been extensively investigated, while their optical properties have been relatively rarely studied. However, the optical constants, e.g., refractive index and extinction coefficient have great importance for waveguiding and other optical applications.

Barium titanate BT is currently one of the most technologically interesting materials due to its large ferroelectric response, high electro-optic coefficient, and second order non-linear susceptibility [1]. Lead zirconate titanate PZT a well known as material for ferroelectric memory applications. High remanent polarization, high dielectric constant, low operating voltage, and low leakage current are attributes of PZT thin films. Thin PZT films have been widely investigated for application in dynamic random access memories (DRAMs) and nonvolatile random access memories (NVRAMs) [2, 3]. PZT is a promising pyroelectric material for infrared sensor application, too [4]. Lead magnesium niobate PMN is the best known and most widely studied relaxor, could be considered as a model object of relaxor materials. Characterized by interesting dielectric, electrostrictive, and piezoelectric properties in single crystal and bulk ceramic forms, PMN thin films are potentially promising candidates for various microelectromechanical applications [5].

In this report optical reflectometry and ellipsometry techniques are combined as an efficient non-destructive tool for measuring thickness, refractive and absorption coefficients of transparent BT, PZT and PMN thin films. Optical constants were determined by fitting the multilayer model function to the measured data.

## 2. Experimental

PMN, BT and PZT thin films were deposited on various substrates $Si(300\ \mu m)/TiO_2(50\ nm)/Pt(100\ nm)Si(300\ \mu m)/SiO_2(1000nm)/Ti(10nm)/Pt(100nm), Si(300\mu m)/TiO_2$

* Corresponding author: ilze@cfi.lu.lv

(50 nm)/Pt(100 nm) by rf-sputtering [6], pulsed-laser deposition (PLD) [7, 15] and sol-gel technique [8-15]. The rf- sputtering was made in collaboration with University of Saarland, Germany, PLD - with Solid state and material research institute in Dresden, IFM-Dresden, Germany and sol-gel technique in the collaboration with Jozef Stefan Institute in Slovenia.

The measurements were performed with variable-angle null-ellipsometer (at He-Ne laser wavelength $\lambda$ = 632.8 nm, angles set from 45° to 75°, step 5°). A miniature "Ocean Optics" CCD spectrometer, model PC 1000, designed as a plug-in PC ISA slot with fiber optics input was used for the reflectivity measurements under normal light incidence geometry in the spectral range of 350 – 750 nm.

Atomic force microscopy (AFM) measurements were performed by Stand Alone SMENA microscope from NT-MDT Co. in contact mode using conventional tips to characterize the surface morphology.

## 3. Results and discussion

Optical constants were determined by fitting experimental data to multilayer model based on matrix formalism. Multilayer system matrix [14] for *p* and *s* polarised light $\tilde{M}_{ij\,s,p} = \tilde{I}_{01s,p}\tilde{L}_1\tilde{I}_{12s,p}\tilde{L}_2 \cdot \ldots \cdot \tilde{I}_{ijs,p}\tilde{L}_j\tilde{I}_{j+1}$, where $\tilde{I}_{ij\,s,p}$ – boundary interface matrix for *p* and *s* polarised light, $\tilde{L}_j$ – layer matrix. Reflective properties for the sample can be ascribed using layer and interface matrix for polarised light $R_p = \tilde{M}_{21p} / \tilde{M}_{11p}$, $R_s = \tilde{M}_{21s} / \tilde{M}_{11s}$ and is connected with main ellipsometric formula $tg\psi\, e^{\Delta} = R_p / R_s$, where $\Psi$ and $\Delta$ - ellipsometric angles. The optical band gap energy of each film was deduced from the spectral dependence of the absorption constant $\alpha(h\nu) = 4\pi k/\lambda$ by applying the Tauc relation [15, 16]:
$\alpha(h\nu) = const\,(h\nu - E_g)^l$, where $l = 1/2$ for a direct allowed transition. By extrapolating the linear part, the optical energy gap was deduced at $\alpha(h\nu)^2$ (Fig 2 a), giving the optical energy gap $E_g$. The optimal values of refractive index, extinction coefficient and thickness for each sample layer were found by Monte Carlo optimisation procedure of multilayer model.

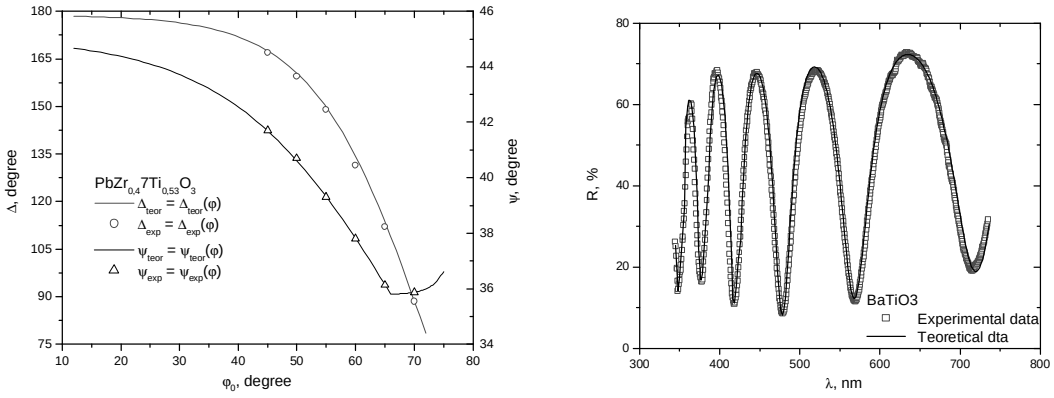


a b

Fig. 1. a) Theoretical and experimental ellipsometric data of PZT, thickness 920nm, sol-gel technique; b) theoretical and experimental reflectometric data of BT, thickness 530nm, PLD technique.

The optical properties at wavelength 632.8 nm and thickness were determined from ellipsometric data. The theoretical and experimental ellipsometric angles $\Psi$, $\Delta$ as a function from the incidence angle $\varphi_0$ are shown on Fig. 1a. Calculated refractive index n, extinction coefficient *k* and *d* from ellipsometric data were taken into account for *n* and *k* dispersion for BT, PZT and PMN thin

films from reflection data. The theoretical and experimental data of reflective index *R* as a function of wavelength is shown on Fig. 1b.

The optical properties of sol-gel PZT and rf-sputtered PMN and PLD BT thin film determined in the phonon energy $E_{ph} = hc/\lambda = h\nu$ range of 1.65 – 3.53 eV (350 – 750 nm) are given on Fig. 2 and 3. As shown in figures the refractive and absorption indexes increase as the phonon energy increase (normal dispersion) what is appropriate for ferroelectric materials in the visible wavelength range. Refractive index and band gap energy for specific PZT composition from the literature in comparison with our work results are given in the Table 1, for PMN and BT in the Tables 2 and 3, respectively. The values in Tables 1, 2 and 3 are obtained from films prepared by different techniques on different substrates, bulk ceramics and crystals. Optical characterisation can be also used as a quality check of thin films. For example, in Ref. 19, the linear variation of the refractive index from PT to PZ, was used to determine the packing densities of the films. The lower refractive index (roughly 5% lower than for ceramics [17] or MOCVD films [18]) is due to 95% packing density of the sol–gel films. In Ref. 30, the increase of the refractive index with increasing annealing temperature was found for RPIB BT films. The refractive index in our work for PZT thin films is in good agreement with Ref. 17 and 20, but band gap energy - with Ref. 22; for PMN – with Ref. 24 and 25, for BT – with Ref. 32 and 33. The differences in the refractive index and band gap energy values (for samples with the same composition) result from variations in the details of the film structure (phase, interface, inhomogeneity, domains, microstructure, top surface or interface roughness) and how these parameters were taken into account in the data analysis.

Table 1. Refractive index values at 632.8nm and band gap energy of PZT ceramics and films.

| Film | *n* | $E_g$, eV | Measurement tech. | Reference |
|---|---|---|---|---|
| PLZT (2/65/35), (8/10/90) ceramics | 2.523; 2.644 | ≈ 3.5 | Ellipsometry | 17 |
| Sol-gel PT, PZT (40/60) | 2.58; 2.45 | ≈ 3.45; 3.60 | Transmittance | 18 |
| MOCVD PZT (20/80), (80/20) on STO, 0.05–1.20 μm | 2.607; 2.505 | - | Prism coupling | 19 |
| PLD PZT 50/50 on (0001) and (1-102) sapphire | 2.54; 2.44 | - | Ellipsometry | 20 |
| FR-sputtering PZT 52/48 on $SiO_2$, $Al_2O_3$, 266 and 259nm | 2.45; 2.50 | - | Transmittance | 21 |
| PZT (x?) on $LaNiO_3/LaAlO_3$ | - | 3.07 | Reflectance | 22 |
| MOCVD PT to PZ on STO, 50 – 100nm, 700 – 1400nm | 2.66 to 2.46 | 3.6 ± 0.1 | Reflectance | 23 |
| Sol-gel PZT 47/53 on Pt, 620nm | 2.55 | 3.11 | Ellipsometry and reflectometry | This work |

Table 2. Refractive index values at 632.8nm and band gap energy of PMN crystals and films.

| Film | n | $E_g$, eV | Measurement tech. | Reference |
|---|---|---|---|---|
| PMNT62/38 crystals | $n_0 = 2.620$ $n_e = 2.601$ | - | Transmittance | 24 |
| PMN 33/67 | 2.56 | 3.35 | Transmittance | 25 |
| FR-sputtering PMN 33/67 on Pt, 770nm | 2.569 | 3.32 | Ellipsometry and reflectometry | This work |

Table 3. Refractive index values of BT and BST films.

| Film | λ(nm), n | $E_g$, eV | Measurement tech. | Reference |
|---|---|---|---|---|
| BT bulk | 550; 2.465 | - | Raman spectrometry | 26 |
| Sol-gel BST 65/35 (1102) $Al_2O_3$, 400 nm | 430 – 1000; 2.16 - 2.35 | 3.48 | Transmittance | 27 |
| Sol-gel BST 90/10 on Si (100), annealed | 480; 1.91 - 2.10 | 4.00 – 4.38 | Transmittance | 28 |
| PLD BST 50/50 on sapphire, 1.08 μm | 633; 2.22 | - | Transmittance | 29 |
| MOSD polycrystalline BT on fused quartz | 550; 2.05 | 3.5 | Transmittance | 30 |
| RPIB BT on Si, annealed, 820 nm – 1180 nm | 633; 1.99 – 2.14 | - | Ellipsometry | 31 |
| PLD BT on quartz, 530 nm | 633; 2.33 | - | Transmittance | 32 |
| FR-sputtering SBT to BT on silicon and Corning glass | 633; ≈ 2.2 – 1.93 ≈ 2.3 – 2.1 | ≈ 3.554 - 2.225 | Ellipsometry and reflectometry | 33 |
| PLD BT on Pt, 320 nm, 170 nm, 130 nm | 633; 2.33, 2.31, 2.35 | 2.86, 3.03, 3.38 | Ellipsometry and reflectometry | This work |

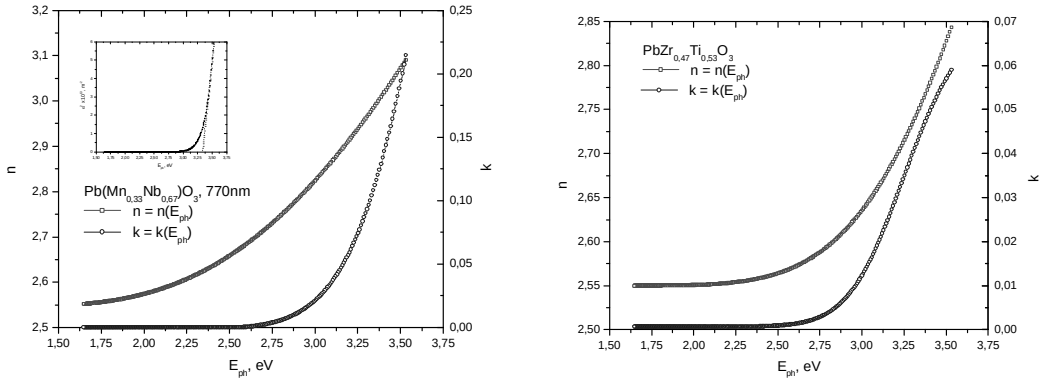


a b

Fig. 2. The refractive index *n* and extinction coefficient *k* for a) PMN, thickness 770 nm, rf-sputtering technique; b) PZT, thickness 920 nm, sol-gel technique.

The variation of refractive index and absorption coefficient has been observed incomparison of PLD BT thin films with different thickness (Fig. 3). The refractive index increase and absorption coefficient shift to the highest photon energies with thickness decrease: estimated band gap energies are 2.86 eV, 3.03 eV and 3.38 eV for film thickness 320 nm, 170 nm and 130 nm respectively. The illustrative pictures of PLD BT thin films surfaces topography with different thickness (340 nm, 170 nm and 130 nm) are given on Fig. 4 a, b and c. With thickness decrease sample surface becomes smoother, but averaged grain size increases in contrary to decreased surface roughness between grains. It was found from AFM images that mean value of maximum-minimum density of grains $R_{mean}$ are 59.4 nm, 35.9 nm, 10.7 nm, root mean square roughness $R_a$ are 20.5 nm, 11.2 nm and 3.2 nm. Observed correlation between optical band gap energy and refractive index changes with the sample surface smoothing and roughness variation are in agreement with Ref. 34, 35. It was found in the

Reference 34 that with increase of deposition temperature and Ba content x in $Ba_xSr_{1-x}Ti_{1.04}O_3$ sample surface become grainier, roughness increase, refractive index and optical band gap decrease. The fundamental absorption edge moves towards to the highest photon energies as observed for $Sr_{1-x}Ba_xTi_{1.04}O_3$ with increase of x, in the Ref. 36. This can be explained by structure and surface morphology changes, which are dependent on the different behavior of Sr or Ba based thin films at the same deposition and annealing temperature. Decreasing of the optical band gap energy and refractive index of $Ba_{0.9}Sr_{0.1}TiO_3$ with increasing of the annealing temperature was observed also in the Ref. 37.

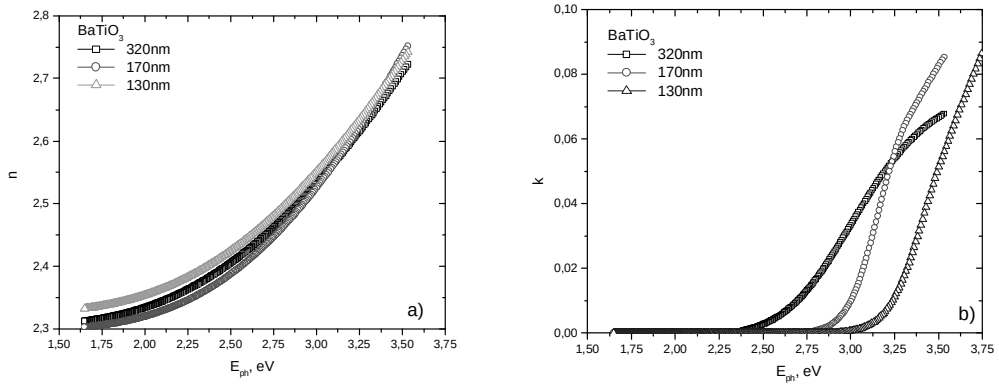


a b

Fig. 3. The refraction coefficient $n$ (a) and extinction coefficient $k$ (b) as the function of the photon energy $E_{ph}$ for BT thin films with different thickness: 530, 320 and 170 nm; PLD deposition technique.

There are no concentration changes and there could not be strong influence of the deposition temperature for our BT thin films. They were deposited with PLD technique at very similar temperature 600 °C and 620 °C, while in the works above deposition temperature changed from 730 °C – 840 °C [34] and 400 °C – 700 °C [37]. These observations suggest that the thin film growing process depends on thickness; as a result it may be responsible for changes in the band structure of the material and for the increased scattering losses due to the surface modifications.

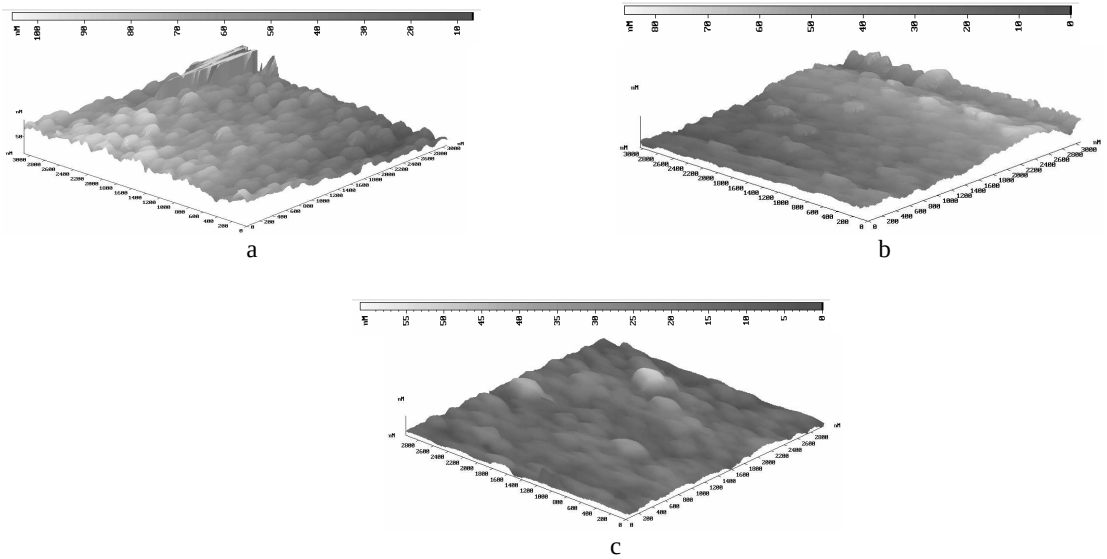

a b c

Fig. 4. Surfaces topography of $BaTiO_3$ thin films with different thickness: a) $d$ = 320 nm, $R_{mean}$ = 59.4 nm, $R_a$ = 20.5 nm, b) $d$ = 170 nm, $R_{mean}$ = 35.9 nm, $R_a$ = 11.2 nm, c) $d$ = 130 nm, $R_{mean}$ = 10.7 nm, $R_a$ = 3.2 nm.

The detailed absorption mechanism is not well understood at present. The impurity may form discrete localized energy levels in the forbidden gap. If its concentration increased sufficiently, the impurity wave functions would overlap to form an impurity band in which the electrons or holes are free to move. These impurities significantly influence the reflective properties of the films and contribute to the fluctuations of the energy level in the internal potential, which would increase absorption beyond the absorption edge in the absorption spectra. Any such defect state can act as a recombination centers if it is capable of trapping a carrier of one type and subsequently capturing a carrier of the opposite type, thereby enabling them to recombine for increasing absorption possibility. On the other hand, oxygen is likely to evaporate thus creating oxygen vacancies, during crystal growth or processing at elevated temperatures. These oxygen vacancies can trap electrons, leading to donor levels in the thin films, which will form indefinite levels in the band gap.

## 4. Conclusions

Ellipsometric measurements at 632.8 nm wavelength in combination with reflectometric spectroscopy at normal incidence in the photon energy range from 1.65 to 3.53 eV have been successfully applied for characterisation of optical properties of BT, PZT and PMN thin films deposited by rf-sputtering, pulsed laser deposition and sol-gel technique. The refractive index and band gap energy was found 2.55 and 3.53 eV for sol- gel deposited PZT films, and 2.569 and 3.32 eV for rf-sputtered PMN thin films, respectively. The variation of refractive index and absorption coefficient has been observed for PLD BT thin films, with different thicknesses. The refractive index slightly decreases and absorption coefficient shifts to higher photon energies with thickness decrease. Estimated values of band gap energies are 2.86 eV, 3.03 eV and 3.38 eV for film thickness 320 nm, 170 nm and 130 nm respectively. The AFM surface topography analysis showed that thin film growth process depends on layer thickness resulting in various surface final roughness patterns and affecting optical properties due to band structure modifications and scattering losses.

**Ackowledgement**

The authors are thankful to L. Cakare (Jozef Stefan Institute) for sol-gel preparation of PZT thin films and C. Ziebert (University of Saarland) for rf-sputtering deposition of PMN thin films. This work was supported by Latvian Council of Science, Excellence Centre of Advanced Material Research and Technology (CAMART) within Institute of Solid State Physics and K. Morberg Scholarship Foundation of University of Latvia.

## References

[1] W. F. Zhang, Y. B. Huang, M. S. Zhanga, Z. G. Liu, Applied Physics Letters, 76, (2000).
[2] F. P. Gnadinger, IEEE VLSI and Computer Peripherals **1**, 20 (1989).
[3] D. Bondurant, F.Gnadinger, IEEE Spectr. **7**, 30 (1989).
[4] G. Suchaneck, T. Sandner, R. Koehler, P. Padmini, G. Gerlach, V. P. Afanasjev, E. V. Tarakanov, ECAPD IV '98/ISAF XI '98/Electroceramics VI '98, Abstract Book, EPFL, Montreux (1998).
[5] H. Y. Wang, Yunzhi Wang, T. Tsakalakos, S. Semenovskaya, A. G. Khachaturyan, Phil. Mag. A **74**(6), 1407 (1996).
[6] H. Schmitt, C. Ziebert, A. Sternberg, V. Zauls, M. Kundzins, K. Kundzins, I. Aulika, K.-H. Ehses, Jan K. Krüger, Ferroelectrics **V268**, 193 (2002)
[7] H. Schmitt, C. Ziebert, A. Sternberg, V. Zauls, M. Kundzins, K. Kundzins, I. Aulika, K. H. Ehses, J. K. Kruger, Ferroelectrics **268**, 193 (2002).
[8] L. Cakare, B. Malic, M. Kosec, Proceedings of 34th International Conference on Microelectronic, Devices and Materials, 349 (1998).
[9] M. Kosec, B. Malic, J. Phys. IV France **8**, Pr9-17- Pr9-26 (1998).

[10] B. Malic, M. Kosec, K. Smolej, S. Stavber, J. of European Ceramic Society **9**, 1345 (1999).
[11] L. Cakare, B. Malic, M. Kosec, A. Sternberg, , Ferroelectrics **241**, 107 (2000).
[12] L. Cakare, B. Malic, M. Kosec, A. Sternberg, Proceedings of NATO Advanced Research Workshop "Defects and Surface-Induced Effects in Advanced Perovskites", Kluwer Academic Publishers, 285 (2000).
[13] A. Sternberg, A. Krumins, K. Kundzins, V. Zauls, I. Aulika, L. Cakare. - Proc. SPIE, **5122**, 345 (2003)
[14] M. Born, E. Wolf, "Principles of Optics Electromagnetic Theory of Propagation, Interference and Diffraction of Light", 7th (expanded) edition, Cambridge University Press (1999).
[15] J. C. Tauc, Optical Properties of Solids, North-Holland, Amsterdam, 372 (1972).
[16] E. A. Davis, N. F. Mott, Phil. Mag. **22**, 903 (1970).
[17] Philips D. Thacher, Appl. Opt. **16**(12), 3210 (1977).
[18] C. H. Peng, J.-F. Chang, S. Desu, Mater. Res. Soc. Symp. Proc. **243**, 21 (1992).
[19] C. M. Foster, G.-R. Bai, R. Csencsits, J. Vetrone, R. Jammy, L. A. Wills, E. Carr, F. Amano, J. Appl. Phys. **81**, 2349 (1997).
[20] S. Trolier-McKinstry, H. Hu, S. B. Krupanidhi, P. Chindaudom, K. Vedam, R. E. Newnham, Thin Solid Films **230**, 15 (1993).
[21] Zhigao Hu, Zhiming Huang, Zhenquan Lai, Genshui Wang, Junhao Chu, Thin Solid Films, in press (2003).
[22] J. D. Klein, S. L. Clauson, Mater. Res. Soc. Symp. Proc. **316**, 147, (1995).
[23] M. P. Moret, M. A. C. Devillers, K. Worhoff, P. K. Larsen, J. Appl. Phys. **92**, 468 (2002).
[24] Xinming Wan, Haiqing Xu, Tianhou He, Di Lin, Haosu Luo, J. APP. PHYS. **93**, 4766 (2003).
[25] Landolt – Bornstein, Ferroelectrics and related substances **16**, 23, Spinger-Verlag, Berlin-Heidelberg, 1981.
[26] S. H. Wemple, J. Chem. Phys. **67**, 2151 (1977).
[27] Tianjin Zhang, Haoshuang Gu, Jianghua Liu, Microelectronic Engineering Microelectronic Engineering **66**, 860 (2003).
[28] Hu-Yong Tian, Wei-Gen Luo, Ai-Li Ding, Jongwan Choi, Changho Lee, Kwangsoo No, Thin Solid Films **408**, 200 (2002).
[29] F. Chelieboum, H. S. Ryu, C. H. Hong, W. S. Park, S. Baik, Thin Solid Films **305**, 20 (1997).
[30] P. C. Joshi, S. B. Desu, Thin Solid Films **300**, 289 (1997).
[31] P. Li, J. F. McDonald, T.-M. Lu, J. Appl. Phys. **71**(ll), 5596 (1992).
[32] W. F. Zhang, Y. B. Huang, M. S. Zhang, Appl. Phys. Lett. 76, 1003 (2000).
[33] B. Panda, A. Dhar, G. D. Nigam, D. Bhattachary, S. K. Ray, Thin Solid Films **332**, 46 (1998).
[34] R. Thielsch, K. Kaemmer, B. Holzapfel, L. Schultz, Thin Solid Films **301**, 203 (1997).
[35] M. Losurdo, D. Barreca, P. Capezzuto, G. Bruno, E. Tondello, Surf. Coat. Tech. **151**, 2 (2002).
[36] P. Pasierb, S. Komornicki, M. Radecka, Thin Solid Films **324**, 134 (1998).
[37] Hu-Yong Tian, Wei-Gen Luo, Ai-Li Ding, Jongwan Choi, Changho Lee, Kwangsoo No, Thin Solid Films **408**, 200 (2002).